

RESEARCH ARTICLE

Dynamic modelling and Chaos control for thin plate oscillator Using Bubnov-Galerkin integral method

Xiaodong Jiao¹ | Jin Tao² | Hao Sun*¹ | Qinglin Sun¹ | Zengqiang Chen¹

¹College of Artificial Intelligence, Nankai University, Tianjin, China

²Silo AI, Helsinki, Finland

Correspondence

*Hao Sun, College of Artificial Intelligence, Nankai University, Tianjin 300350, China.
Email: sunh@nankai.edu.cn

Present Address

College of Artificial Intelligence, Nankai University, Tianjin 300350, China.

Abstract

Thin plate system based on acoustic vibration plays an important role in micro nano manipulation and exploration of nonlinear science. In this paper, starting from the actual thin plate system driven by acoustic wave signals, combining the mechanical analysis of thin plate micro element and the approximation approach Bubnov-Galerkin integral method, the governing equation of a forced vibration square thin plate is derived. Of note, the reaction force of the thin plate vibration system is defined as $f = \alpha |w|$ resembling the Hooke's law. And then by solving amplitude-frequency response function of the thin plate oscillator using the harmonic balance method, the amplitude-frequency curves under the action of distinct parameters are analyzed with two different vibration modes through numerical simulation. Further, the conservative chaotic motions in the thin plate oscillator is demonstrated by the theory and numerical method. Drawing the dynamics maps indicating the system states reveals the evolution laws of the system. Through expounding the effect of force fields and system energy, the underlying mechanism of chaos is interpreted. Additionally, the phenomenon of chaos occurred in the oscillator is controlled by the method of velocity and displacement states feedback, which is meaningful for the engineering application.

KEYWORDS:

Thin plate oscillator, Conservative chaos, Bubnov-Galerkin method, Frequency response, Chaos control

1 | INTRODUCTION

The micro thin plate system driven by acoustic waves has been extensively used in some important engineering fields, such as microchip assembly^{1,2}, cell culture^{3,4,5} and particle manipulations^{6,7,8}. These tasks make full use of the advantages of acoustic manipulation based on vibration plate including 1):miniaturization of control equipment, 2):contactless manipulation, 3):diversity of manipulation targets and experiment environment compatibility. And the physical principle behind these acoustic manipulation is Chladni effect, which is discovered in 1787 by German physicist Ernst Florens Friedrich^{9,10}. Apparently, the structures of the thin plate, material and geometric properties will closely influence the manipulation accuracy of the thin plate system. On the other hand, from the driving signal source, amplitude and frequency, even the driving interval are all the important factors that will influence the effect of micro thin plate. Consequently, it has both theoretical value and practical meaning to investigate the micro thin plate vibration system by acoustic waves.

Simultaneously, nonlinear oscillators of various types attract a lot of attentions as they play an important role in many engineering technology and industrial production. Some nonlinear oscillators with typical characteristics have been investigated in recent years. Such as Zhou and Chen reported the Rayleigh-Duffing oscillator with no-smooth periodic perturbation and harmonic excitation¹¹. Gendelman, O, Kravets, P et al, studied a forced vibro-impact oscillator with coulomb friction¹². The chaotic motions of a simple dry-friction oscillator is investigated by Licsko and Csernak¹³. Li et al demonstrated the nonlinear impact oscillators with bilateral rigid constraints¹⁴. With particular emphasis, micro thin plate oscillators are also an important branch as their promising and valuable prospects in various application scenarios. Dynamic analysis of amplitude frequency characteristics is the most key indicator reflecting the oscillator performances. In which, the resonance region and resonance frequency with maximum system energy under different parameter and geometric conditions can be determined to guide and adjust the practical application.

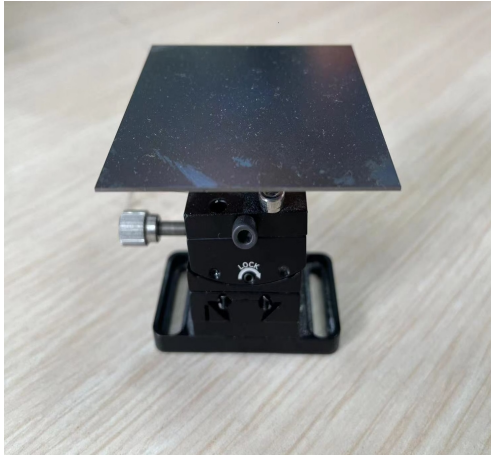
Moreover, chaotic dynamics of the nonlinear vibration systems have also been discussed in recent years for its inevitability. Zhou and Chen investigated the chaotic motions of the Rayleigh-Duffing oscillator^{11,15}. In¹⁶, Meleshenko, P. A. et al reported the conservative chaos in a simple oscillatory system with non-smooth nonlinearity. Boudjema, R. investigated the dynamical manifestation of chaotic behavior in a q-Tsallis harmonic oscillator¹⁷. Alliluev A. D. and Makarov D. V. analyzed the dynamics of a Nonlinear Quantum oscillator under Non-Markovian pumping¹⁸. Kruglov, V. P, Krylosova, D. A, Sataev, I. R, et al revealed the features of a chaotic attractor in a quasiperiodically driven nonlinear oscillator. Alternatively, there are many ways to characterize the chaotic property of a dynamic system¹⁹. The intuitive method for determining the occurrence of chaos is to draw the phase portrait and the sequence diagram, and observe the complexity and disorder of their evolution laws. Further more, by calculating the Lyapunov exponents(LEs) of a dynamic system and judging their positive and negative to determine the state of system, and the characteristic of a conservative system is summarized as zero-sum LEs, but the non-conservative system with negative-sum LEs^{20,21,22,23,24}. Meanwhile, the dynamic evolution characteristics is another important aspect of analysis by the improved method. In this paper, the thin plate oscillator is transformed into a three-dimensional autonomous system. The conservative chaotic characteristics of proposed oscillator is revealed through theoretical analysis and simulation verification, as well as the evolution process by drawing and concluding the dynamics maps based on the various parameters and initial values.

Throughout the relevant reports of chaos research, modeling from the actual background is of great significance, which will help to further guide the practical engineering. Whereas, there is a lack of research and analysis on chaos mechanism. Very recently, researchers have made some contributions. One of the universal methods is analyzing the action effects of force fields and energy in the system progressively. For instance, Pelino, V et al reveal the energy cycle for the Lorenz attractor²⁵. Yang, Y, Qi, G et al analysis the mechanism of plasma chaotic system combining mechanics and energy²⁶. Similarly, the underlying reason for the chaos of thin plate oscillator modeled in this paper is also explored. When it comes to the applications of chaotic systems, generally, the randomness of chaotic sequence is considered, which includes secure communication, image encryption, fault identification of the system, signal prediction and stock financial fields^{27,28}. Chaos means that in a deterministic system, there is a seemingly random irregular motion, and its behavior is uncertain, unrepeatable and unpredictable. Unfortunately, the phenomenon of chaos is not expected in many engineering projects. That is because chaotic vibration will probably cause the instability of an actual system. And the uncontrolled instability is the main inducement for system damage or crash and low efficiency. Chaotic vibration will make the system produce irregular oscillation, often produce some unpredictable interference fluctuations, resulting in mechanical load exceeding its bearing range, excessive increase of noise and reduction of operation accuracy. Hence, chaotic phenomena need to be avoided in some engineering applications. The control target is to effectively obtain the periodic orbit needed or suppress the chaotic behavior through possible strategies and methods^{29,30,31,32}. As a result, the effective suppression and control of chaos have significant practice meaning. Chaos generated in the proposed thin plate oscillator is controlled by the state feedback method.

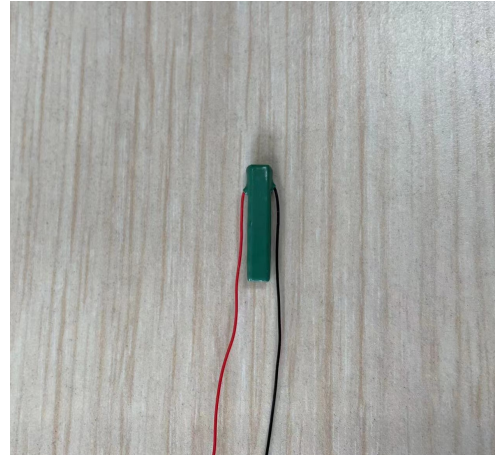
The rest of this paper is arranged as the following order: in Section 2, by mechanical analysis and mathematical derivation, the system governing equation of the thin plate oscillator is obtained. In Section 3, the relationship of amplitude-frequency response is solved by the method of harmonic balance method(HBM), and the amplitude-frequency curves are drawing to analysis the effects of various parameters and different vibration modes on amplitude-frequency characteristic. And then, conservative chaotic property in the proposed oscillator is demonstrated by mathematical verification and numerical simulation in Section 4, and by computing the dynamics maps analyzing the evolution process and laws of the system. Further, the chaos mechanism is expound by analyzing the effects of force fields and energy progressively. Meaningfully, the appeared chaos is controlled by the state feedback. Finally, some conclusions are given in the last Section.

2 | SYSTEM GOVERNING EQUATION

As an important mean of non-contact acoustic manipulation³³, revelation of complex dynamics behaviors of vibrating thin plate system plays a great practical value in some engineering problems. In this paper, the modeling analysis is based on the physical thin plate as shown in the Fig.1(a). The Silicon thin plate is fixed on a Piezoelectric actuator (shown as Fig.1(b)) and driven by sinusoidal signal source, and the two axis slider is used to adjust the horizontal position of the plate. Driven by different acoustic waves, the thin plate oscillator will vibrate variously, such as the chaotic vibration and regular vibration reflected by microparticles shown in Fig.1(c-d). In this working system, the chaotic vibration is undesirable and needs to be controlled, but the regular motion is favorable. Therefore, chaotic phenomenon in this system needs to be controlled or suppressed.



(a) Physical thin plate.



(b) Piezoelectric actuator.



(c) Disordered vibration mode.



(d) Regular vibration mode.

FIGURE 1 The thin plate vibration system.

The forced vibration thin plate undergoes small displacements. What is the rationale behind the displacements, essentially, the conditions that complex stress of the system play a decisive role. Homoplastically, the geometry and material properties of the thin plate are also the key factors for the vibration deflection of thin plate. In this paper, on the basis of Kirchhoff-Love thin plate theory, fully considering the stress conditions of the thin plate, the governing equation for a thin plate system is formulated as Eq.(1). Notably, the form of the external load p and the reaction force f will directly affect the dynamic characteristics of the vibration thin plate system.

$$D\nabla^4 w + \rho h \frac{\partial^2 w}{\partial t^2} + \mu \frac{\partial w}{\partial t} = f + p(x, y, t) \quad (1)$$

in which ∇^4 is the double Laplace operator, defined as $\nabla^4 = \nabla^2(\nabla^2 w)$, D is the bending rigidity of plate, ρ is the plate density, h is the plate thickness. $p(x, y, t)$ is the external drive mechanism with the form that , and A , ω , φ are amplitude, frequency and phase respectively of the driving signal. It is particularly worth mentioning, for a thin plate of elastic materials under the external excitation, the reaction force is considered as $f = \alpha |w|$ which is defined by analogy with Hooke's law in this system, and α indicates the coupling strength of thin plate and driver.

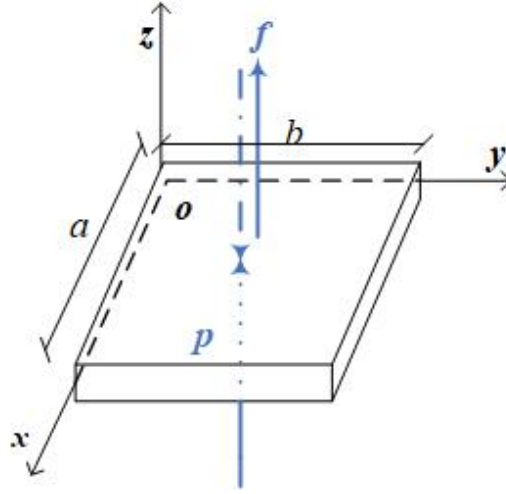


FIGURE 2 Diagram of simply supported thin plates on four edges.

The following boundary conditions should be met for a simply supported square thin plate.

$$w \Big|_{x=0} = 0, w \Big|_{x=l} = 0, w \Big|_{y=0} = 0, w \Big|_{y=l} = 0 \quad (2)$$

$$\frac{\partial^2 w}{\partial x^2} \Big|_{x=0} = 0, \frac{\partial^2 w}{\partial x^2} \Big|_{x=l} = 0, \frac{\partial^2 w}{\partial y^2} \Big|_{y=0} = 0, \frac{\partial^2 w}{\partial y^2} \Big|_{y=l} = 0 \quad (3)$$

Accordingly, the midplane deflection function of square thin plate is assumed as

$$w(x, y, t) = \sum_{m=1}^{\infty} \sum_{n=1}^{\infty} q_{mn}(t) \sin\left(\frac{m\pi x}{l}\right) \sin\left(\frac{n\pi y}{l}\right) \quad (4)$$

of note, m, n are positive integers, l is the side length of square thin plate.

The residual function R for the forced vibration dynamic equation (1) is

$$R[w, x, t] = D\nabla^4 w + \rho h \frac{\partial^2 w}{\partial t^2} + \mu \frac{\partial w}{\partial t} - f - p(x, y, t) \quad (5)$$

Substitute Eq.(4) into Eq.(5), one gets

$$\begin{aligned} R[w, x, t] = & D\nabla^4 \sum_{m=1}^{\infty} \sum_{n=1}^{\infty} q_{mn}(t) \sin\left(\frac{m\pi x}{l}\right) \sin\left(\frac{n\pi y}{l}\right) + \rho h \sum_{m=1}^{\infty} \sum_{n=1}^{\infty} \ddot{q}_{mn}(t) \sin\left(\frac{m\pi x}{l}\right) \sin\left(\frac{n\pi y}{l}\right) \\ & + \mu \sum_{m=1}^{\infty} \sum_{n=1}^{\infty} \dot{q}_{mn}(t) \sin\left(\frac{m\pi x}{l}\right) \sin\left(\frac{n\pi y}{l}\right) - \alpha \left| \sum_{m=1}^{\infty} \sum_{n=1}^{\infty} q_{mn}(t) \sin\left(\frac{m\pi x}{l}\right) \sin\left(\frac{n\pi y}{l}\right) \right| - p(x, y, t) \end{aligned} \quad (6)$$

For a two-dimensional thin plate continuum, the Bubnov-Galerkin integral method is applied, furnishes

$$\int_0^a \int_0^b \sin\left(\frac{m\pi x}{a}\right) \sin\left(\frac{n\pi y}{b}\right) \left\{ D \nabla^4 \sum_{m=1}^{\infty} \sum_{n=1}^{\infty} q_{mn}(t) \sin\left(\frac{m\pi x}{a}\right) \sin\left(\frac{n\pi y}{b}\right) + \rho h \sum_{m=1}^{\infty} \sum_{n=1}^{\infty} \ddot{q}_{mn}(t) \sin\left(\frac{m\pi x}{a}\right) \sin\left(\frac{n\pi y}{b}\right) \right. \\ \left. + \mu \sum_{m=1}^{\infty} \sum_{n=1}^{\infty} \dot{q}_{mn}(t) \sin\left(\frac{m\pi x}{a}\right) \sin\left(\frac{n\pi y}{b}\right) - \alpha \left| \sum_{m=1}^{\infty} \sum_{n=1}^{\infty} q_{mn}(t) \sin\left(\frac{m\pi x}{a}\right) \sin\left(\frac{n\pi y}{b}\right) \right| - p(x, y, t) \right\} dx dy = 0 \quad (7)$$

in which, $a = b = l$.

After partial derivative calculation and integration, the ordinary differential equation of the square thin plate vibration system is cast in the form

$$\pi^4 D \left[\frac{m^2 + n^2}{l^2} \right] q_{mn}(t) + \rho h \ddot{q}_{mn}(t) + \mu \dot{q}_{mn}(t) = \alpha |q_{mn}(t)| + P_{mn}(t) \quad (8)$$

with $D = \frac{Eh^3}{12(1-\nu^2)}$, E and ν , respectively, indicate the Young's modulus and the Poisson's ratio,

$$P_{mn}(t) = \int_0^a \int_0^b \sin\left(\frac{m\pi x}{a}\right) \sin\left(\frac{n\pi y}{b}\right) p(x, y, t) dx dy.$$

As a result, differential equation of forced vibration of square thin plate is organized as

$$\pi^4 D \left[\frac{m^2 + n^2}{l^2} \right] q_{mn}(t) + \rho h \ddot{q}_{mn}(t) + \mu \dot{q}_{mn}(t) = \alpha |q_{mn}(t)| + \frac{4l^2}{mn\pi^2} A \cos(\omega t) \quad (9)$$

3 | ANALYSIS OF AMPLITUDE-FREQUENCY RESPONSE

In this section, the amplitude-frequency response of system (9) is derived by the method of harmonic balance method, and a lot of numerical simulations are performed. As consequence, some conclusions that closely affect the amplitude frequency characteristics are obtained, which is of vital significance for the vibration control of square thin plate system. Forced vibration state is the response of the system to vibration under the action of continuous and uninterrupted excitation force. When the excitation source is removed, the vibration is transformed into free vibration based on natural frequency. The system response under simple harmonic excitation is consist of transient response and steady-state response. During the steady-state response, the vibration frequency of the system is the same as that of the excitation force. When the frequency of the excitation force is close to the natural frequency of the system, the vibration amplitude suddenly increases, that is, resonance occurs. In some cases, the physical phenomenon of resonance will bring harm to mankind. However, in many cases, people can skillfully use it to serve mankind. Hence, the amplitude-frequency characteristic is an important research content of oscillator.

3.1 | Amplitude-frequency response

Relabel the coefficients of Eq.(9) for simplifying, one gets

$$m \ddot{q}_{mn}(t) + \mu \dot{q}_{mn}(t) + K_1 q_{mn}(t) = \alpha |q_{mn}(t)| + K_2 \cos(\omega t) \quad (10)$$

in which $m = \rho h$, $K_1 = \pi^4 D \left[\frac{m^2 + n^2}{l^2} \right]$, $K_2 = \frac{4l^2}{mn\pi^2} A$.

Applying the harmonic balance method, the relationship of amplitude-frequency response can be solved as follows.

The response function is considered as

$$x = a \cos(\omega t + \varphi) \quad (11)$$

And rewrite the external incentive force of the system as

$$p(x, y, t) = A \cos(\omega t) \\ = A \cos(\varphi) \cos(\omega t + \varphi) + A \sin(\varphi) \sin(\omega t + \varphi) \quad (12)$$

Then, substitute the Eq.(11), Eq.(12) in the dynamic system Eq.(10), and consider the positive $\cos(\omega t + \varphi)$, the following equations is derived

$$\begin{cases} -ma\omega^2 + aK_1 - \alpha |a| = K_2 \cos(\varphi) \\ -\mu a\omega = A \sin(\varphi) \end{cases} \quad (13)$$

Square both sides of the Eq.(13) and add them separately, consequently, one gets

$$(-ma\omega^2 + aK_1 - \alpha |a|)^2 + (-\mu a\omega)^2 = K_2^2 \quad (14)$$

The relationship of amplitude-frequency response is organized as

$$a = K_2 * (K_1^2 + m^2\omega^4 - 2K_1m\omega^2 + \alpha^2 - 2K_1\alpha + 2m\omega^2\alpha + \mu^2\omega^2)^{-\frac{1}{2}} \quad (15)$$

3.2 | Amplitude-frequency curves

In order to study the influence of system parameters to the amplitude-frequency response, numerical simulations are calculated to summarize the evolution law of amplitude-frequency response for the proposed oscillator. This paper focuses the effects under the distinct sheet thickness h , sheet side length l , amplitude of external excitation force A and vibration modes (m, n) . For all simulation conditions, the material parameters are set according to Silicon, which has a density 2329g/m^3 , a Young's modulus of $170 * 10^9\text{ Pa}$, and a Poisson's ratio of 0.28, and $\mu = 0.2, \alpha = 1$.

Case1: Analysis of the sheet thickness h

In this case, the amplitude-frequency response curves are computed with different sheet thickness h and under the vibration modes $(m=1, n=1)$, $(m=1, n=3)$. Other parameters are selected as, sheet side length $l=0.1\text{m}$, excitation amplitude $A=100$.

From the amplitude-frequency response curves with distinct color shown in Fig.3(a, b), in which, the plate thickness are selected as $h=0.2\text{mm}$, $h=0.4\text{mm}$ and $h=0.6\text{mm}$ respectively for different vibration modes $(m=1, n=1)$ and $(m=1, n=3)$. From Fig.3(a, b), the conclusion is that with the increase of plate thickness, the amplitude of thin plate decreases, inversely, the resonance frequency is increasing. The vibration mode changes from $(m=1, n=1)$ to $(m=1, n=3)$, but the amplitude decreases. For engineering application, it suggested that the thinner plates and higher order vibration modes are considered to avoid large resonance amplitude causing damage to the sheet system.

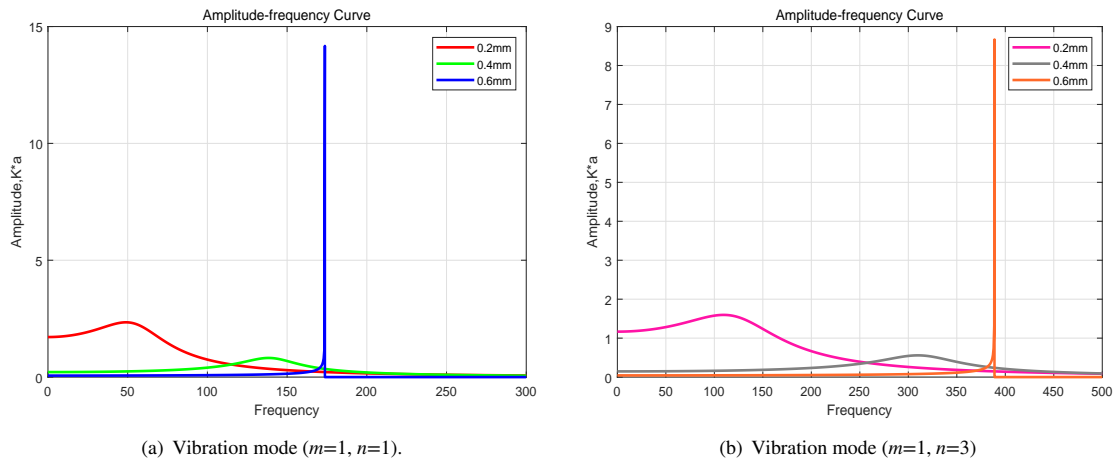


FIGURE 3 Amplitude frequency characteristics under different vibration modes (m,n) and plate thickness (h) .

Case2: Analysis of the side length l

In Case2, based on the equation of amplitude-frequency response, the effect of the sheet side length l is simulated. The side length l of the square thin plate are set as $l=5\text{cm}$, $l=10\text{cm}$ and $l=15\text{cm}$ for vibration modes $(m=1, n=1)$ and $(m=1, n=3)$ separately. The plate thickness is fixed as 0.2mm , excitation amplitude $A=100$. And the corresponding amplitude-frequency response curves are shown in Fig.4(a, b), with the increase of the side length of the thin plate, the amplitude of the thin plate also increases. Instead, the resonance frequency becomes smaller, concurrently, the resonance amplitude is increasing. In addition, the resonance frequency will enlarge with the increase of vibration mode evidently.

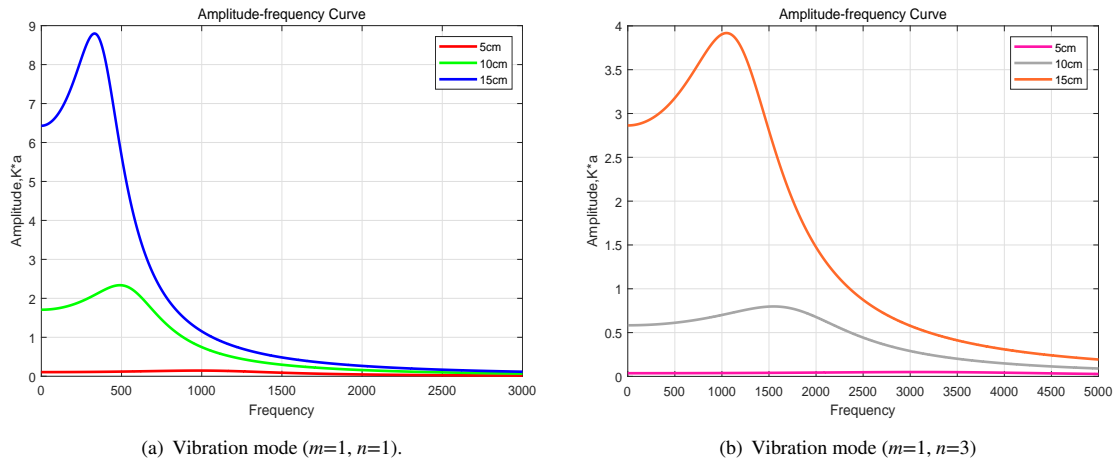


FIGURE 4 Amplitude frequency characteristics under different vibration modes(m,n) and side length(l).

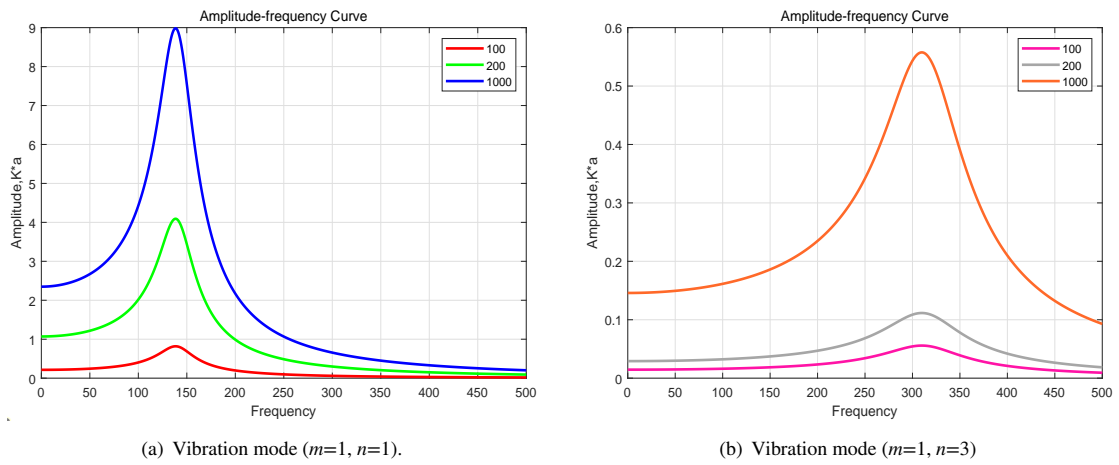


FIGURE 5 Amplitude frequency characteristics under different vibration modes(m,n) and side length(A).

Case3: Analysis of the excitation amplitude A

The influence of the excitation amplitude A is analyzed in this case. The sheet thickness and the sheet side length, separately, are chosen as $h=0.4\text{mm}$, $l=0.1\text{m}$. Amplitude-frequency response curves are shown in Fig.5(a, b) for the vibration modes $(m=1, n=1)$, $(m=1, n=3)$.

According to the simulation results, the excitation amplitude A will not transform the resonance frequency but the vibration amplitude increases. Other parameter settings remain unchanged, the resonance frequency increases with the increase of vibration mode. Hence, excitation amplitude A is an crucial factor to adjust the vibration amplitude of thin plate, which are important application index in vibration system.

By analyzing the amplitude frequency response under different vibration conditions and vibration modes, some practical conclusions can be obtained and further guide the application of vibration system, which closely related to the selection of vibrating thin plate properties and adjustment of excitation force in engineering application. Summarize from the above three type simulations, keeping other conditions unchanged, the increase of vibration mode will reduce the vibration amplitude of thin plate vibration system. As consequence, referring to the results of the above analysis, the damage of vibration system can be avoided and improve the application efficiency of vibration system.

4 | CHAOTIC PROPERTY AND ITS CONTROL

The phenomena of chaos exist extensively in all kinds of nonlinear systems, and apparently, chaos is inevitable in the vibration system^{34,35}. Where, the conservative chaos is rarely reported. The behavior of dynamic system in chaotic state shows strong randomness. In some industrial production fields, such as chemical reaction and meteorological prediction, secret communication, chaotic systems are advantageous and needed. Nevertheless, in the thin plate oscillator, chaos should be avoided to ensure the stability and safety of the system. Generally, the methods for chaos controlling are divided into feedback control and non feedback control. Consequently, the chaotic phenomenon in the proposed thin plate oscillator is analyzed in detail through theoretical and numerical simulation, and which is also controlled based on the method of state feedback.

4.1 | Conservative chaos and dynamic evolution

Conservative chaos can be determined by Lyapunov exponents and the phase space trajectory of the system. In Eq.(9), the relationship between the vibration response of the thin plate and the parameters is described. Simplify the system parameters and relabel the variables, one gets the state equation form of system (9) as

$$\begin{cases} \dot{x} = y \\ \dot{y} = a|x| + b \cos(\omega t) - cy - dx \end{cases} \quad (16)$$

in which, x indicates the generalized displacement, and y means the generalized velocity. Set $z = \omega t$, a three-dimensional autonomous dynamic system (17) can be obtained

$$\begin{cases} \dot{x} = y \\ \dot{y} = a|x| + b \cos(z) - cy - dx \\ \dot{z} = \omega \end{cases} \quad (17)$$

the corresponding Jacobian matrix is

$$J = \begin{bmatrix} 0 & 1 & 0 \\ a \operatorname{sign}(x) - d & -c & -b \sin(z) \\ 0 & 0 & 0 \end{bmatrix}. \quad (18)$$

When the initial values x_0, y_0, z_0 are set as (0.2, 100, 0.05), the parameters are set as $a=2, b=300, c=0.001, n=1.5, d=2.1$. The proposed dynamic system (17) presents chaotic characteristic because the Lyapunov exponents is calculated as +0.0512, 0.0000, -0.0522 shown in Fig.6(a). Using the results of Lyapunov exponents of the three-dimensional autonomous dynamic system (17), the Lyapunov dimension can be obtained by

$$D_L = 2 + \frac{L_1 + L_2}{|L_3|}. \quad (19)$$

as a result, $D_L = 2.98 \approx 3$, the calculation results tend to integer, which also shows the conservative chaotic characteristics of the system.

Simultaneously, the divergence of system (17) can be calculated according to

$$\nabla V = \frac{\partial \dot{x}}{\partial x} + \frac{\partial \dot{y}}{\partial y} + \frac{\partial \dot{z}}{\partial z} = 0 + c + 0 \quad (20)$$

consequently, the degree of dissipation for system (17) is determined by the value of parameter c , in this proposed chaotic state, $c=0.001$, which is close to 0, that means the volume of phase space of system (17) is constant, and the spatial trajectories are neither divergent nor convergent. Combined with the calculation results of Lyapunov exponents (+,0,-), Lyapunov dimension (tend to integer, $2.98 \approx 3$), divergence (approximate to 0), the chaotic phenomenon with all these characteristics can be classified as the conservative chaos. And the corresponding chaotic attractor is displayed in Figs.6(b), which is formed by complex spatial trajectories and shows the chaotic property of the proposed thin plate oscillator.

In addition, the evolution process of dynamic system directly reflects the characteristics of the system. For the purpose of investigating the dynamic evolution process, the dynamics maps of system(17) is drawn with various parameter and initial condition. As system(17) is a three dimensional dynamic system, meanwhile, there is always 0 LE during the calculation process to keep the stability of the system. Thus, the first LE is a key indicator reflecting the dynamic evolution process. In which, the positive first LE indicates the chaotic motion, inversely, the negative or zero first LE represent the regular motion of the system.

Based on the first LE, the dynamics maps for system(17) are shown in Figs.7(a-b). With the steps of 0.1, the variable parameter and initial value in Fig.7(a) are $a \in [0, 10], x_0 \in [5, 15]$, and Fig.7(b) are $b \in [-5, 5], z_0 \in [-5, 5]$ respectively. From Fig.7(a),

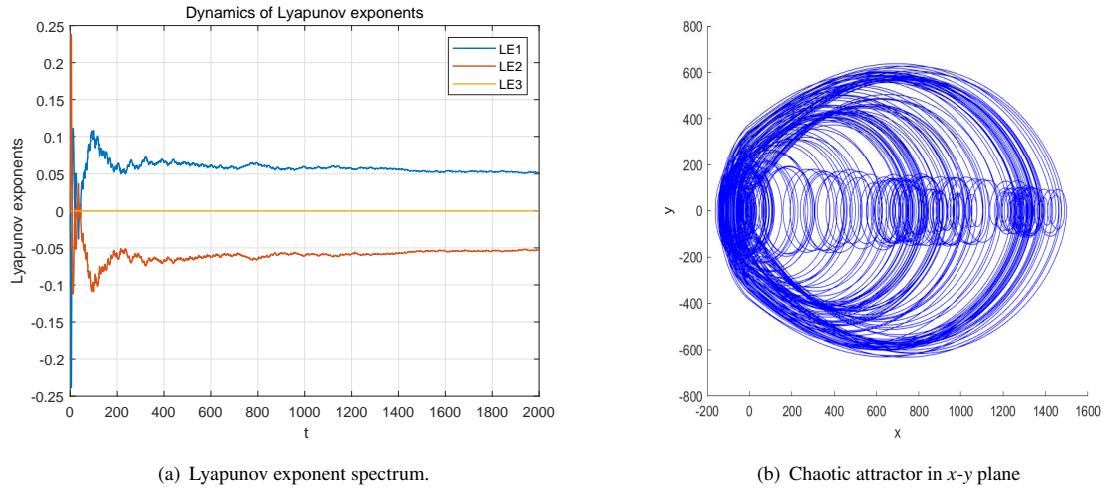


FIGURE 6 Chaotic property of system (17).

the region of yellow surface refers to the chaotic states with the positive first LE, other region shows the regular motion with the negative first LE. Concurrently, the change of x_0 does not affect the system evolution process, but the system will evolve differently with the change of parameter a . Fig.7(b) displays the dynamic evolution with varying b and z_0 , from which, the evolution process is depicted by the calculation results first LEs. From Fig.7(b), the dynamic evolution process is symmetry about the parameter axis $b = 0$. Simultaneously, the system evolves in various degrees under changing b and z_0 according to the color bar, the areas marked red have higher randomness, but the areas marked blue have lower randomness. The method of drawing dynamics maps provides an useful tool to analyze the evolution law of the system based on the parameter and initial condition intuitively.

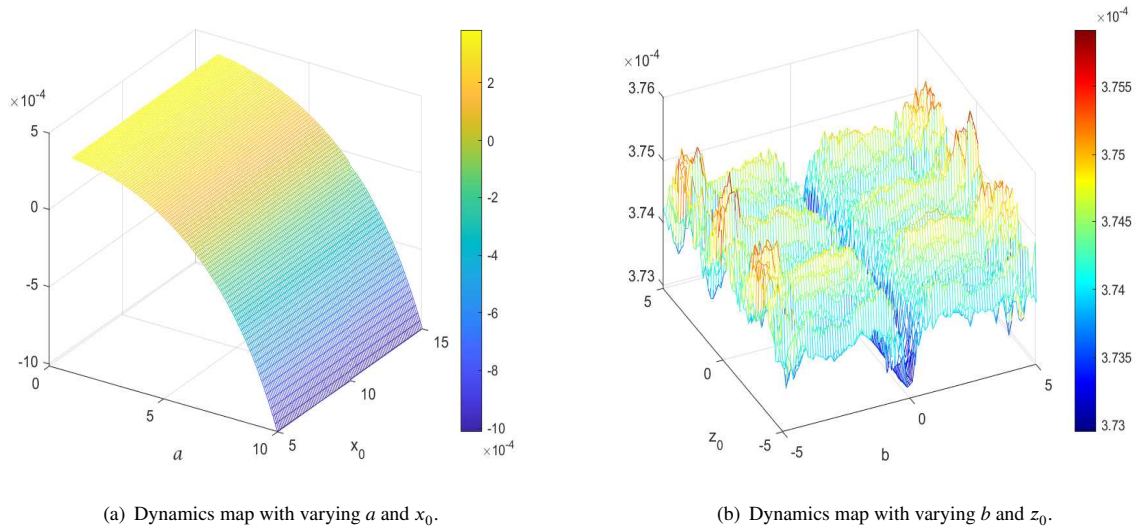


FIGURE 7 Dynamics map of system(17) with varying parameters and initial values.

4.2 | Analysis of chaos mechanism

Any chaotic or hyperchaotic systems can be represented by the generalized Hamiltonian system, which can be described as the Kolmogorov type further. In this way, the dynamic system is decomposed into three force fields including conservative force field, dissipative force field and external force field. And then, by analyzing the effect of these force fields acting on the system and the variation of system energy, the mechanism of the emergence of chaos could be explained. Accordingly, system (17) has the following form

$$\dot{x} = \{x, H\} + f_d + f_e \quad (21)$$

Go a step further

$$\{x, H\} = \begin{bmatrix} y \\ a|x| - dx \\ 0 \end{bmatrix}, f_d = \begin{bmatrix} 0 \\ -cy \\ 0 \end{bmatrix}, f_e = \begin{bmatrix} 0 \\ b \cos(z) \\ \omega \end{bmatrix} \quad (22)$$

in which, $\{x, H\}$ is the conservative force field, the dissipative force field is indicated by f_d , f_e means the external force field. As consequence, the chaotic mechanism of the proposed thin plate oscillator can be analyzed gradually. The system parameters and initial conditions are also set as sub-section 4.1.

Firstly, only the conservative force $\{x, H\}$ works on the system, the system keeps energy conservation, there is no energy exchanged between the inside and outside of the system. Thus, the system has the stable evolution. Combined with the numerical simulations shown in Figs.8(a-b), the corresponding phase space portrait is a closed periodic ring, and the state variable of the system change uniformly. Next, the dissipative force is added, in this case, the conservative characteristic of the system is destroyed, and the spatial trajectory of the system becomes quasi-periodic shown in Figs.9(a) instead of the simple periodic motion. Under the condition of long enough time, the system will gradually dissipate as the time history curve shown in Figs.9(b). Finally, the external force f_e is also added. All the force fields exert on the system. And especially, owing to the external force f_e , there is energy exchanged between the inside and outside of the system. Consequently, chaos appears in the system due to the fluctuation of system energy. As the chaotic attractor in three-dimensional space shown in Fig.10(a). And the time history curve of variable x in Fig.10(b) shows disorder. In a word, the effect of force fields and system energy provide an useful channel for explaining the occurrence of chaos in the thin plate oscillator.

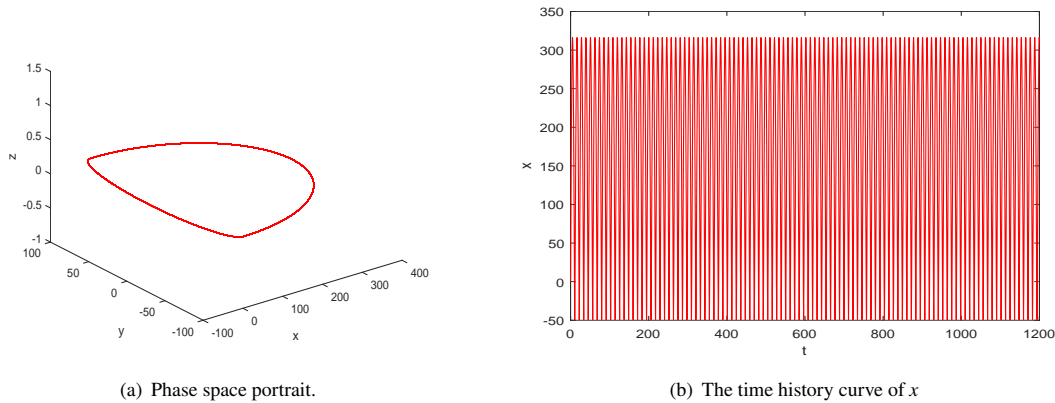


FIGURE 8 Only the conservative term works.

4.3 | Chaos control based on state feedback

The dynamic motion resulted by chaos is violent oscillation. Unfortunately, the appearance of chaos will make the system undergo an unstable state, whereas in the actual project, that is harmful. Engineers hope the system work steadily on the steady-state to avoid any bifurcation and chaotic behavior. Chaos control is to make the controlled chaotic system break away from the chaotic state and achieve the expected periodic dynamic behavior, such as equilibrium state, periodic motion or quasi periodic motion^{36,37}. The goal of chaos control is to eliminate the bifurcation behavior and chaos of the system. As consequence, fast

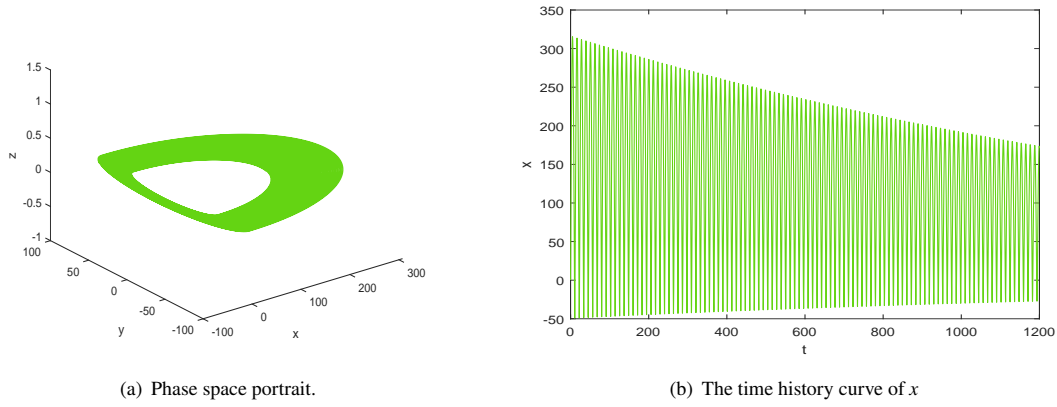


FIGURE 9 Add dissipative term.

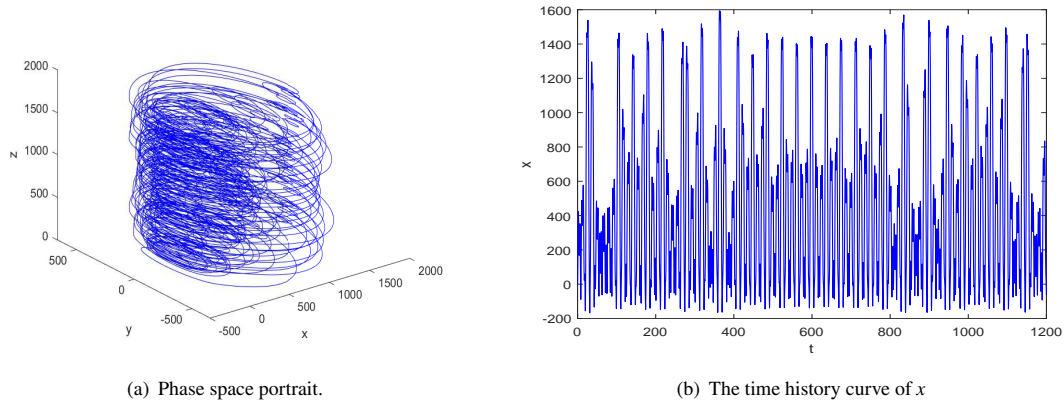


FIGURE 10 Conservative, dissipative and external force terms work.

suppression of chaos is a control task in engineering. Chaos control mainly refers to eliminate chaos and suppress the occurrence of chaos, which means to stabilize the system to the desired equilibrium point or periodic state.

In sub-section 4.1, the conservative chaotic property of the proposed thin plate oscillator, a class of chaos with higher randomness, is analyzed in detail. The method of state feedback is used to suppress the chaos in this sub-section. For system (17), the displacement feedback controller u_1 and velocity feedback controller u_2 are designed to control the chaos appeared in last sub-section. Under the action of the controllers, the governing equation of the system becomes

$$\begin{cases} \dot{x} = y + u_1 \\ \dot{y} = a|x| + b\cos(z) - cy - dx + u_2 \\ \dot{z} = \omega \end{cases} \quad (23)$$

in which, the controllers are set as $u_1 = -k_1x$, $u_2 = -k_2x$. Set the system parameters according to sub-section 4.1, let $u_2 = 0$, and the displacement state feedback u_1 is set as $u_1 = -2x$. The governing equation of system becomes

$$\begin{cases} \dot{x} = y - 2x \\ \dot{y} = a|x| + b\cos(z) - cy - dx \\ \dot{z} = \omega \end{cases} \quad (24)$$

The spatial trajectory and time series of variable x are obtained through simulations, as shown in the Figs.11(a-b). From the simulation results, the spatial trajectory in x - y plane shown in Fig.11(a) is a purple closed curve illustrating that the control result

is periodic state, and the time series are changing regularly and evenly as the light blue sequence diagram shown in Fig.11(b), which show that the chaotic behavior of the system is effectively eliminated under the action of the displacement feedback controller u_1 .

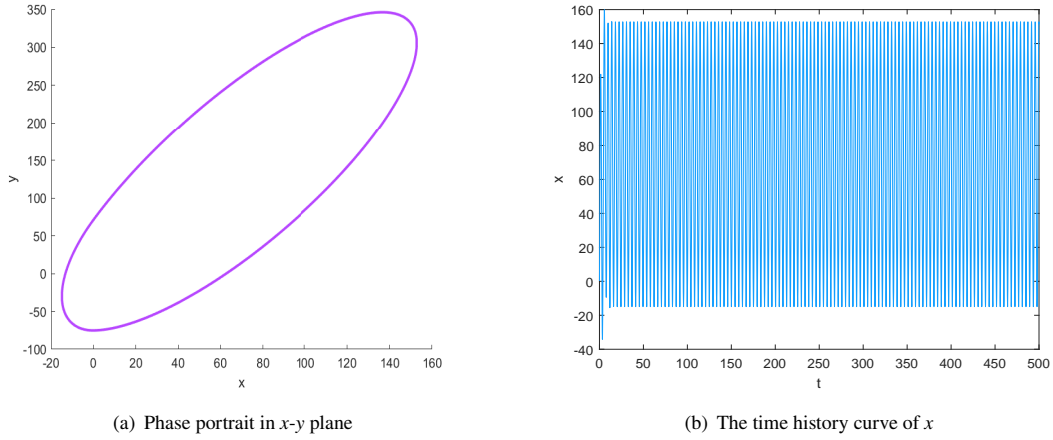


FIGURE 11 Control results of the displacement feedback controller u_1 .

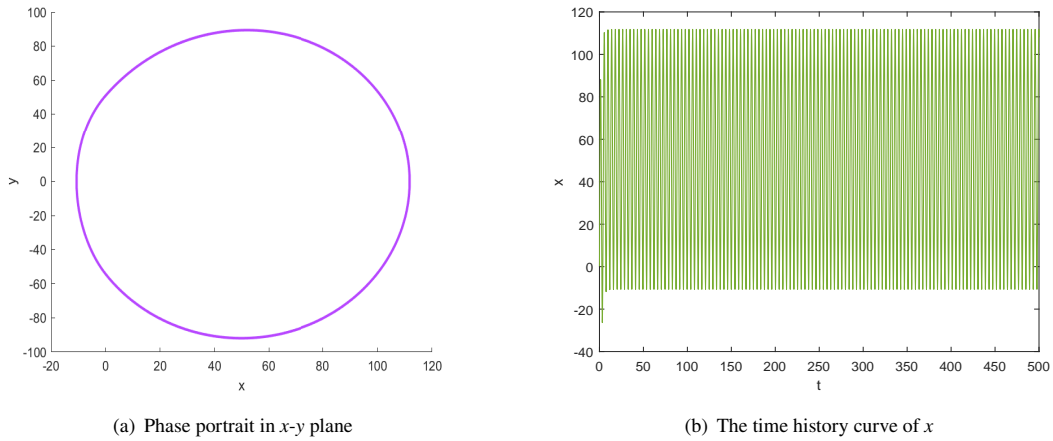


FIGURE 12 Control results of the velocity feedback controller u_2 .

And next, let $u_1 = 0$, and the velocity state feedback u_2 is set as $u_2 = -3y$. The governing equation of system becomes

$$\begin{cases} \dot{x} = y \\ \dot{y} = a|x| + b\cos(z) - cy - dx - 3y \\ \dot{z} = \omega \end{cases} \quad (25)$$

Accordingly, the phase portrait and time series of variable x are shown in the Figs.12(a-b). From the simulation results above, the phase portrait and the time series explain the periodic state of system (25), which also verify the effectiveness of the designed velocity feedback controller u_2 for controlling the chaotic behavior of the proposed thin plate oscillator.

5 | CONCLUSIONS

The thin plate system driven by acoustic waves has a promising application prospect in the fields of micro nano manipulation, tissue culture and self-assembly. In this paper, a micro thin plate vibration system driven by the acoustic waves is modeled and analyzed comprehensively. Firstly, the governing equation of the system is obtained by analyzing the mechanical conditions of thin plate micro element and detailed mathematical derivation. Secondly, solving the amplitude-frequency response function of the thin plate oscillator and drawing the corresponding amplitude-frequency curves, the influences of three different system parameters and two vibration modes on amplitude frequency characteristics are summarized to further guide the practical application. And the phenomenon of the conservative chaotic motions appeared in the thin plate oscillator is revealed utilizing mathematical calculation and numerical simulations. For analyzing the evolution process of the system, the evolution laws are illustrated by drawing the dynamics maps. And then, explicate the occurrence of chaos through analyzing the effect of force fields and system energy. Finally, designing the displacement and velocity state feedback controllers, the control of chaos is performed, with the results of periodic state to further avoid the inexpectant engineering damages.

ACKNOWLEDGMENTS

This work was supported by the National Natural Science Foundation of China(Grant No.61973172, 62003177, 62103204, 62003175 and 61973175).

Financial disclosure

None reported.

Conflict of interest

The authors declare no potential conflict of interests.

References

1. Chen P, Luo Z, Tasoglu S. Microscale Assembly Directed by Liquid-based Template. *Advanced Materials* 2014; 26(34): 5936-5941.
2. Fujita Y, Ishihara S, Nakashima Y. Selective Transfer of Si Thin-Film Microchips by SiO₂ Terraces on Host Chips for Fluidic Self-Assembly. *Appl. Mech* 2021; 2(1): 16-24.
3. Monterosso M, Futrega K, Lott WB. Using the Microwell-mesh to culture microtissues in vitro and as a carrier to implant microtissues in vivo into mice. *Scientific Reports* 2021; 11(1): 5118.
4. Tmaa B, Ga A, Frt A. Mass spectrometry-based proteomics of 3D cell culture: A useful tool to validate culture of spheroids and organoids. *SLAS Discovery* 2022; 27(3): 167-174.
5. Khademhosseini A, May M, Sefton M. Conformal coating of mammalian cells immobilized onto magnetically driven beads. *Tissue Engineering Part A* 2005; 11(11-12): 1797-1806.
6. Dai H, Xia B, Yu D. Microparticles separation using acoustic topological insulators. *Applied Physics Letters* 2021; 119(11): 11601-.
7. Am A, Nai A, Vmf A. Transport and assembling microparticles via Marangoni flows in heating and cooling modes. *Colloids and Surfaces A: Physicochemical and Engineering Aspects* 2021; 621: 126550 - 126550.
8. Snezhko A, Aranson I. Magnetic Manipulation of self-assembled colloidal asters. *Nature Materials* 2011; 10: 698-703.

9. Luo Y, Feng R, Li X, Liu D. A simple approach to determine the mode shapes of Chladni plates based on the optical lever method. *European Journal of Physics* 2019; 40: 065001.
10. Tuan P, Wen C, Chiang P, Yu Y. Exploring the resonant vibration of thin plates: Reconstruction of Chladni patterns and determination of resonant wave numbers. *Journal of the Acoustical Society of America* 2015; 137: 2113-2123.
11. Zhou L, Chen F. Chaos of the Rayleigh-Duffing oscillator with a non-smooth periodic perturbation and harmonic excitation. *Mathematics and Computers in Simulation* 2021; 192(C): 1-8.
12. Gendelman O, Kravets P, Rachinskii D. Mixed global dynamics of forced vibro-impact oscillator with Coulomb friction. *Dynamical Systems (math.DS)* 2019: 1-17.
13. Licsko G, Csernak G. Chaos and transient chaos in a simple oscillator with Coulomb friction law. *IEEE International Conference on Nonlinear Science and Complexity* 2012; IEEE.
14. Li S, Wu H, Zhou X. Theoretical and experimental studies of global dynamics for a class of bistable nonlinear impact oscillators with bilateral rigid constraints. *International Journal of Non-Linear Mechanics*; 2021(1450022): 103720.
15. An X. Chaos prediction in the Duffing-type system with non-smooth periodic perturbation and bounded parametric excitation. *Acta Physica Sinica* 2008; 57(12): 7535 - 7540.
16. Meleshenko P, Semenov M, Klinskikh A. Conservative chaos in a simple oscillatory system with non-smooth nonlinearity. *ACS Applied Bio Materials Nonlinear Dynamics* 2020; 101(4): 2523 - 2540.
17. Boudjema R. Dynamical Manifestation of Chaotic Behaviour in a q-Tsallis Harmonic Oscillator. *International Journal of Theoretical Physics* 2022; 61(3): 1-13.
18. Alliluev A, Makarov D. Dynamics of a Nonlinear Quantum Oscillator Under Non-Markovian Pumping. *Biomechanics Journal of Russian Laser Research* 2022; 43(1): 71-81.
19. Kruglov V, Krylosova D, Sataev I. Features of a chaotic attractor in a quasiperiodically driven nonlinear oscillator. *Chaos* 2021; 31(7): 073118.
20. Vaidyanathan S, Volos C. Analysis and adaptive control of a novel 3-d conservative no-equilibrium chaotic system. *Arch. Control Sci.* 2015; 25(3): 1-21.
21. Jia I, Shi W, Wang L. Energy analysis of Sprott-A system and generation of a new Hamiltonian conservative chaotic system with coexisting hidden attractors. *Chaos Solitons and Fractals* 2020; 133: 109635.
22. Cang S, Li Y, Kang Z. A generic method for constructing n -fold covers of 3D conservative chaotic systems. *Chaos* 2020; 30(3): 033103.
23. Singh J, Rajagopal K, Roy B. Switching between Dissipative and Conservative Behaviors in a Modified Hyperchaotic System with the Variation of Its Parameter. *International Journal of Bifurcation and Chaos* 2021; 31(16): 2130048.
24. Zhang K, Chen M, Wang Y. Dynamic Analysis and Degenerate Hopf Bifurcation-Based Feedback Control of a Conservative Chaotic System and Its Circuit Simulation. *Complexity* 2021; 2021(3): 1-15.
25. Pelino V, Maimone F. Lorenz cycle for the Lorenz attractor. *Chaos Solitons and Fractals the Interdisciplinary Journal of Nonlinear Science and Nonequilibrium and Complex Phenomena* 2009; 64: 67-77.
26. Yang Y, Qi G. Mechanical analysis and bound of plasma chaotic system. *Chaos Solitons and Fractals* 2018; 108: 187-195.
27. Tlelo-Cuautle E, Gerardo D, Pham V. Dynamics, fpga realization and application of a chaotic system with an infinite number of equilibrium points. *Nonlinear Dynamics* 2017; 89: 11291139.
28. Bahi J, Fang X, Guyeux C. FPGA Design for Pseudorandom Number Generator Based on Chaotic Iteration used in Information Hiding Application. *Applied Mathematics and Information Sciences* 2013; 7(6): 2175-2188.

29. Vaidyanathan S, Azar A. A Novel 4-D Four-Wing Chaotic System with Four Quadratic Nonlinearities and Its Synchronization via Adaptive Control Method. *Springer International Publishing* 2016; 337: 203-224.
30. Luo S, Ma H, Li F. Dynamical analysis and chaos control of MEMS resonators by using the analog circuit. *Nonlinear Dynamics* 2022; 108(1): 97-112.
31. Din Q, Ishaque W, Iqbal M. Modification of Nicholson's Bailey model under refuge effects with stability, bifurcation, and chaos control,. *Journal of Vibration and Control* 2021; 2021(3): 107754632110340.
32. Makouo L, Tsafack K, Tingue M. Synchronization and Chaos Control Using a Single Controller of Five Dimensional Autonomous Homopolar Disc Dynamo,. *International Journal of Robotics and Automation* 2021; 2021(3): 19-31.
33. Hu J. An introduction to acoustic micro/nano manipulations. *Applied Physics* 2016; 6: 114-118.
34. Yang D, Zhou J. Connections among several chaos feedback control approaches and chaotic vibration control of mechanical systems. *Communications in Nonlinear Science and Numerical Simulation* 2014; 19(11): 3954-3968.
35. Nbandjo B, Tchoukuegno R, Wofo P. Active control with delay of vibration and chaos in a double-well Duffing oscillator. *Chaos Solitons and Fractals* 2003; 18(2): 345-353.
36. Yavari M, Nazemi A, Mortezaee M. On chaos control of nonlinear fractional chaotic systems via a neural collocation optimization scheme and some applications. *New Astronomy* 2022; 94: 101794-.
37. Selvam A, Jacob S, Dhineshababu R. Bifurcation and Chaos Control for Prey Predator Model with Step Size in Discrete Time. *Journal of Physics: Conference Series* 2020; 1543(1): 012010.

